A Simple Modified Peak Detection Based UWB Receiver for WSN and IoT Applications

Sanjeev Sharma[1], Anubha Gupta[2], Senior Member, IEEE and Vimal Bhatia[1], Senior Member, IEEE
[1] SaSg, Discipline of Electrical Engineering,
Indian Institute of Technology Indore, India 453552, {phd1501102011,vbhatia}@iiti.ac.in
[2] SBILab, Department of Electronics and Communication Engg.,
Indraprastha Institute of Information Technology-Delhi, New Delhi-110020, anubha@iiitd.ac.in

***Abstract*—Ultra-wide band (UWB) communication is a viable solution for Wireless Sensor Network (WSN) and Internet of Things (IoT) due to low cost and low power requirement. However, UWB transceiver design is more complex due to large bandwidth and precise synchronization requirement. In this paper, we propose a simple peak detection based non-coherent UWB receiver, suitable for low data rate WSN and IoT based applications. The proposed receiver divides each data symbol frame duration into smaller multiple time windows. In each time window, peak of received signal is detected independently using threshold comparison. The transmitted signal is detected in a frame by employing decisions on all multiple time windows. From simulation, it is observed that the proposed receiver outperforms existing non-coherent receivers. The performance analysis of the proposed receiver is carried out by using time hopping pulse position modulation (TH-PPM) UWB signal in additive white Gaussian noise (AWGN), multipath communication using the existing IEEE 802.15.4a standard.**

***Index Terms*—UWB Communication, Wireless Sensor Network, Internet of Things, Peak Detection, Non-coherent Receiver.**

I. Introduction

Ultra-wide band (UWB) unlicensed frequency band technology can be used in high data rate wireless communications in local and personal area networks, wireless sensor networks (WSN) and, location and ranging in Internet of Things (IoT) due to low power and low cost technology [1–6]. In WSN and IoT based applications, transceivers should be designed with low power consumption and less circuit complexity. Currently, researchers are exploring UWB in IoT based applications using simple system implementation [1–3, 7]. UWB communication can also be used to connect various air interfaces at physical layer in 5G communication and high data rate (up to 100x gigabits per second) wireless local area networks at millimeter wave communications due to the availability of wide spectrum at high frequencies (above 28 GHz) [8, 9].

UWB radio-frequency identification (RFID) devices can be designed for real-time locating systems (RTLSs) for long battery life [10]. UWB not only support higher data rate but also consumes very low power, which is an essential requirement in WSN and IoT that require connecting billions of devices together. UWB can also be used in IoT applications using upcoming standard IEEE 802.11ah, called "Wi-Fi HaLow", which will use unlicensed frequencies around 2.4 GHz and 5 GHz bands to overcome the limitation of Wi-Fi and ZigBee standards. Power consumption, interference minimization, and high-definition localization are some important aspects in WSN and IoT that can be addressed using UWB [10]. UWB is also proposed for wireless health monitoring based applications using IEEE 802.15.6 standard that can be very helpful for patients monitoring for smart home in IoT.

In the UWB literature, both coherent and non-coherent receivers are proposed. The performance of coherent receivers is better than the non-coherent receiver. However, coherent receivers have more system implementation complexity. Coherent receivers e.g. matched or correlation based UWB receivers are complex and require high sampling rate [11]. Therefore, these receivers are not suitable for low cost and low power IoT based applications.

Transmitted-reference (TR) non-coherent receiver is yet another type of receiver for low data rate communications. TR receiver does not require complex channel estimation method. However, it requires long analog delay line to store the reference signal that is not practical in the current technology. Non-coherent energy detector based UWB receiver also exists that does not require channel estimation and uses simple hardware circuitry. However, non-coherent energy detector based receivers degrade system performance, especially, in low signal-to-noise ratio (SNR) regime. In order to overcome this drawback, weighted energy detectors (WED) are proposed in the literature [12, 13] to enhance the system performance.

Simple energy detectors require squarer, mixers, and integrating devices. Weighted energy detectors require training phase for finding the optimal weights. This makes the system more complex and inappropriate for WSN and IoT applications. In [4], power requirement analysis of energy detector is carried out in RFID and WSN applications. Passive RFID tag localization has been proposed in [5] for green communication using UWB communication. An improved energy detector is also designed in [14] for implantable biomedical devices. Therefore, the above literature highlights the use of UWB in WSN and IoT applications with low power system designs.

In this paper, we explore UWB application in WSN and IoT applications using the IEEE 802.15.4a standard [15, 16]. We propose a new peak detection receiver for simple and low power consuming UWB communication receiver for low or medium data rate IoT and WSN based applications. The proposed receiver divides the data symbol frame duration into

smaller multiple time windows and the peak of the signal is detected in each window time interval using threshold technique. Finally, transmitted signal is detected based on the total number of peaks in each data symbol frame duration.

The peak detection receiver works on the instantaneous value of signal and noise. Therefore, performance of peak detection receiver does not degrade compared to energy detector and has a very simple implementation. The proposed receiver does not require mixer, squarer, and integrating blocks. Hence, it has low implementation cost and less power consumption as compared to energy detector. Low power requirement is desirable in WSN and IoT based applications in order to increase long battery life. Therefore, the proposed receiver can be a preferable solution for low data rate WSN and IoT applications.

Further, the proposed peak detection receiver reduces synchronization complexity that is required in energy detector for reducing noise effect. The proposed receiver is analyzed using time hopping pulse position modulation (TH-PPM) UWB system. To verify the robustness of the proposed receiver, TH-PPM UWB system performance is analyzed in additive white Gaussian noise (AWGN) and multipath communication channels.

The paper is organized as follows: In Section II, basic UWB system model for TH-PPM signal is described. The proposed peak detection receiver is discussed in Section III. Simulation and discussions on results are presented in Section IV. Finally, some conclusions are drawn in Section V.

II. System Model

In this section, we describe UWB system model for TH-PPM signal. The combined signal $w_c(t)$ of N_f consecutive frames using UWB pulse $w(t)$ of duration T_w for data symbol $d_k \in \{0, 1\}$ is represented as

$$w_c(t) = \sum_{j=0}^{N_f-1} \sqrt{E_w} w(t - jT_f - c_j T_c - \delta_{\text{PPM}} d_k), \quad (1)$$

where T_f is the frame duration, E_w is the pulse energy calculated as $E_w = \int_{-\infty}^{\infty} w^2(t)dt$, c_j is the random time hopping (TH) code of cardinality N_h and period N_p, T_c is the chip time duration, and δ_{PPM} is the pulse position modulation (PPM) index.

In this paper, δ_{PPM} is considered as half of the frame duration T_f. Signal $s(t)$ corresponding to k^{th} transmitted data symbol d_k of the TH-PPM UWB system can be written as

$$s(t) = \sum_{k=0}^{\infty} w_c(t - kT_s), \quad (2)$$

where $T_s = N_f T_f$ is the data symbol duration. Thus, signal $s(t)$ incorporates UWB pulse in the first or second halves of frame duration T_f depending upon the data symbol $d_k = 0$ or $d_k = 1$, respectively.

Received signal $r(t)$ is expressed as

$$r(t) = s(t) \otimes h(t) + n(t), \quad (3)$$

where '$\otimes$' is the linear convolution operator and $h(t)$ is the channel impulse response, which has L number of multipaths and expressed as $h(t) = \sum_{l=0}^{L-1} \alpha_l \delta(t - \tau_l)$, where $\{\alpha_l\}_{l=0}^{L-1}$ and $\{\tau_l\}_{l=0}^{L-1}$ are channel coefficients and path delays, respectively. $n(t)$ is AWGN of zero mean and σ^2 variance.

Further, we have assumed $\delta > T_c + T_h$ to avoid inter-symbol interference (ISI) effect in the system, where T_h is the non-zero time duration of the channel.

III. Proposed Peak Detection Receiver

In this section, we present the proposed non-coherent peak detection based UWB receiver. This receiver based on signal peak detection is simple and less power consuming compared to the coherent receivers. In the proposed receiver design, each time frame T_f is divided into smaller multiple time windows. Peak of the received signal is calculated in each window time interval. The received signal of j^{th} frame in i^{th} window interval $W_{ij}(t)$ can be written as $W_{ij}(t) = r(t - jT_f - iT_b)$, where $i = 1, 2, ..., M, \quad M = \lfloor T_f/2T_b \rfloor$, T_b is the window time duration, and $\lfloor \cdot \rfloor$ is a floor function.

Let $d_k = 0$ is the data symbol being transmitted. Corresponding received signal in smaller multiple time windows is written as $W_{ij,0}(t) = r(t - jT_f - iT_b)$ and $W_{ij,1}(t) = r(t - jT_f - iT_b - \delta_{\text{PPM}})$, where $W_{ij,0}(t)$ and $W_{ij,1}(t)$ are time windows in the first and second halves of j^{th} data frame of duration T_f, respectively. $\{W_{ij,0}(t)\}_{i=1}^{M}$ and $\{W_{ij,1}(t)\}_{i=1}^{M}$ represent disjoint time intervals of the received signal. Assuming zero ISI, $\{W_{ij,0}(t)\}_{i=1}^{M}$ represents signal plus noise and $\{W_{ij,1}(t)\}_{i=1}^{M}$ represents only noise corresponding to the data symbol $d_k = 0$.

The proposed peak detection receiver architecture is shown in Fig.1. Each frame duration T_f is divided into two equal time periods corresponding to data symbols $d_k = 0$ and $d_k = 1$, respectively. Further, each half of the frame is divided into smaller time windows $W_{ij,\ell}, i = 1, ..., M, \ \ell = 0, 1$. The peak of received signal is detected independently in each smaller time window $W_{ij,\ell}$.

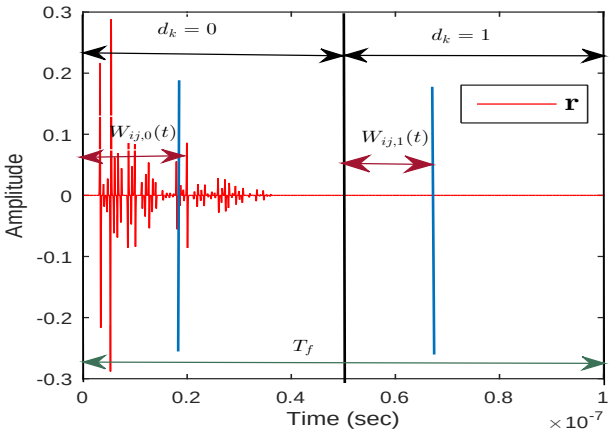

Fig. 1. The j^{th} frame architecture of the proposed peak detection receiver.

We consider discrete-time signal sampled at Nyquist rate. Received signal $r(t)$, transmitted signal $s(t)$, channel

impulse response $h(t)$, UWB pulse $w(t)$, and AWGN $n(t)$ are represented by vectors as $\mathbf{r} = \left[r(0), r(1), ..., r(K-1)\right]^T$, $\mathbf{s} = \left[s(0), s(1), ..., s(K-1)\right]^T$, $\mathbf{h} = \left[h(0), h(1), ..., h(K-1)\right]^T$, $\mathbf{w} = \left[w(0), w(1), ..., w(K-1)\right]^T$ and $\mathbf{n} = \left[n(0), n(1), ..., n(K-1)\right]^T$, respectively, where K is the total number of samples at Nyquist rate in a fixed time duration and $[\cdot]^T$ represents the transpose of $[\cdot]$.

Let the received signal has *N* discrete samples in the window time interval T_b. Received signal $r_g = s_g + n_g, g = 1, 2, ..., N$ in windows $\{W_{ij,0}(g)\}_{i=1}^{M}$ has Gaussian distribution of s_g mean and $2\sigma^2 B$ variance, where *B* is the bandwidth of receiver filter and s_g and n_g, $g = 1, 2, ..., N$ are the received signal and noise in T_b time duration, respectively. Hence, distribution of signal r_g in each window interval $W_{ij,0}(g)$ is distributed as $\mathcal{N}(s_g, 2\sigma^2 B)$. Similarly, we can write the distribution of signal r_g in each window $W_{ij,1}(g)$ as $\mathcal{N}(0, 2\sigma^2 B)$. The desired signal s_g value can be different in each time interval window T_b due to the multipath nature of channel.

For each window time interval, we have calculated peak value of the received signal. The peak value of received signal in each window is calculated using threshold comparison of the received signal. The peak of received signal is detected if absolute value of any sample of received signal in window duration T_b is greater than some threshold V_{th}. Similar, peak of signal is absent if absolute value of any sample of received signal in window duration T_b is less than threshold V_{th}. The peak detection probability for data symbol $d_k = 0$ in the first half of frame duration can be written as

$$p_{peak,d,W_{ij,0}} = p(r_g = s_g + n_g \geq V_{th} \cap r_g \leq -V_{th}), g = 1, ..., N, \tag{4}$$

where $p_{peak,d,W_{ij,0}}$ represents the peak detection probability in the window duration $W_{ij,0}(g)$. Equation (4) can be re-written as

$$\begin{aligned} p_{peak,d,W_{ij,0}} &= p(|r_g| \geq V_{th}), \ g = 1, ..., N \\ &= 1 - p(|r_g| < V_{th}), \ g = 1, ..., N \\ &= 1 - \prod_{g=1}^{N} \int_{-V_{th}}^{V_{th}} \frac{1}{\sqrt{2\pi 2\sigma^2 B}} \exp\left(-\frac{(x - s_g)^2}{4\sigma^2 B}\right) dx \end{aligned}$$

$$p_{peak,d,W_{ij,0}} = 1 - \prod_{g=1}^{N} \left[1 - Q\left(\frac{s_g + V_{th}}{\sqrt{2\sigma^2 B}}\right) - Q\left(\frac{-s_g + V_{th}}{\sqrt{2\sigma^2 B}}\right)\right], \tag{5}$$

where $Q(\cdot)$ represents the tail probability of normal Gaussian function. The peak detection probability for data symbol $d_k = 0$ in the second half of frame duration is also calculated using multiple time windows $\{W_{ij,1}(g)\}_{i=1}^{M}$. The peak detection probability $p_{peak,d,W_{ij,1}}$ in each window $W_{ij,1}(g)$ is expressed as

$$\begin{aligned} p_{peak,d,W_{ij,1}} &= p(|r_g = n_g| > V_{th}), g = 1, ..., N \\ p_{peak,d,W_{ij,1}} &= 1 - \prod_{g=1}^{N} \left[\int_{-V_{th}}^{V_{th}} \frac{1}{\sqrt{2\pi 2\sigma^2 B}} \exp\left(-\frac{x^2}{4\sigma^2 B}\right) dx\right] \end{aligned}$$

$$p_{peak,d,W_{ij,1}} = 1 - \prod_{g=1}^{N} \left[1 - 2Q\left(\frac{V_{th}}{\sqrt{2\sigma^2 B}}\right)\right]. \tag{6}$$

The total peak detection probability $p_{peak,d,0}$ in the first half of frame duration T_f is given as

$$p_{peak,d,0} = \sum_{i=1}^{M} p_{peak,d,W_{ij,0}}, \tag{7}$$

and the total peak detection probability $p_{peak,d,1}$ in the second half of frame duration is given as

$$p_{peak,d,1} = \sum_{i=1}^{M} p_{peak,d,W_{ij,1}}. \tag{8}$$

In Fig. 2, we have simulated (7) and (8) for various window interval and SNR values by considering data symbol $d_k = 0$. At SNR=20 dB, the threshold value (V_{th}) around 0.18 can distinguish between data symbols $d_k = 0$ and $d_k = 1$ due to the higher probability of the (7) as compared to the (8) as shown in Fig. 2. However, at SNR=0 dB probability distinction is low between data symbols $d_k = 0$ and $d_k = 1$ as compared to SNR=20 dB for particular threshold value. Further, probability graphs are distinguished for various window time durations as observed in Fig. 2. The window interval corresponding higher probability for given threshold can be selected for the better system performance.

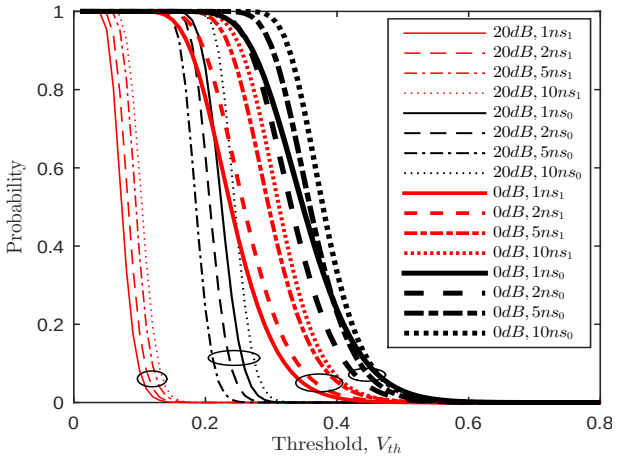

Fig. 2. The average probability vs threshold V_{th} plot. The "$(\cdot)ns_0$" and "$(\cdot)ns_1$" represent (7) and (8) respectively, and results are simulated for two SNR values ($SNR = 0, 20$ dBs) and 1, 2, 5, 10 ns window intervals.

Further, the peak detection probability in each smaller window time interval can be weighted using some optimum weights for better system performance in the proposed receiver design. The difference of peak detection probability $p_{peak,d}$ between first and second halves of frame duration T_f corresponding to data symbol $d_k = 0$ is given by

$$p_{peak,d} = p_{peak,d,0} - p_{peak,d,1}. \tag{9}$$

Data symbol can be demodulated according to the sign of peak detection probability $p_{peak,d}$, where the estimated data symbol

$\hat{d}_k$ mapping is given as below.

$$\hat{d}_k = \begin{cases} 0, & \text{if } p_{peak,d} \geq 0 \\ 1, & \text{otherwise} \end{cases}$$

Further, when the data symbol $d_k = 0$ is transmitted, the error probability $p(e|\mathbf{h}, d_k = 0)$ for a given channel realization $\mathbf{h}$ of the proposed peak detection receiver is given by

$$p(e|\mathbf{h}, d_k = 0) = p(p_{peak,d} < 0)$$
$$p(e|\mathbf{h}, d_k = 0) = p(p_{peak,d,0} < p_{peak,d,1})$$
$$p(e|\mathbf{h}, d_k = 0) = p(\sum_{i=1}^{M} p_{peak,d,W_{ij,0}} < \sum_{i=1}^{M} p_{peak,d,W_{ij,1}}) \quad (10)$$

Equation (10) can be re-written as (11). Similar to (11), the error probability $p(e|\mathbf{h}, d_k = 1)$ when data symbol $d_k = 1$ is transmitted is given as in (12).

The bit error rate (BER) $p(e|\mathbf{h})$ when all symbols are equally likely can be written as

$$p(e|\mathbf{h}) = \frac{1}{2}p(e|\mathbf{h}, d_k = 0) + \frac{1}{2}p(e|\mathbf{h}, d_k = 1). \quad (13)$$

The BER in (13) depends upon the threshold value V_{th} and channel realization $\mathbf{h}$. The optimal value of threshold V_{th} can be set as $V_{th} = 0.6 \max_g\{|s_g|\}$ [17], however, it is not optimum for a range of SNR. The unconditional BER $p(e)$ is calculated using ensemble averaging over multiple channel realizations and is expressed as

$$p(e) = \frac{1}{Z}\sum_{z=1}^{Z} p(e|\mathbf{h}_z), \quad (14)$$

where Z is the total number of channel realizations and $\mathbf{h}_z$ is the z^{th} channel realization.

IV. Simulation and Discussion

In this section, we have carried out simulations to verify the proposed peak detection UWB receiver design. Simulation results have been generated for TH-PPM UWB system using first order modified Hermite polynomial (MHP) as a transmitted UWB pulse $\mathbf{w}$ in single user environment. The transmitted pulse $\mathbf{w}$ in analog domain can be written as [18]

$$w(t) = A\left(\frac{t}{\eta}\right)\exp\left(-t^2/4\eta^2\right), \quad t \in \mathbb{R} \quad (15)$$

where A is the pulse amplitude parameter that limits the transmitted pulse energy and η is the pulse width parameter with $\eta = 0.07$ nanoseconds (ns). The TH code c_j is generated using $N_h = 3, 7$ and $N_p = 100$ for AWGN and multipath channels, respectively. Chip duration $T_c = 1$ ns is considered, SNR is defined as $SNR = E_w/\sigma^2$, sampling frequency is 30 GHz, and BER curves are generated using ensemble averaging over 100 realizations.

The average BER performance of TH-PPM UWB system using the proposed receiver and the energy detector receiver [11, 19] in AWGN channel is shown in Fig. 3. The frame duration $T_f = 20$ ns and $N_f = 1$ are considered for AWGN channel results. The proposed receiver outperforms energy detector by ≈ 3 dBs for $T_b = 1$ ns as observed from Fig. 3. The effect of window duration T_b is also analyzed and results are shown in Fig. 3. As window duration increases, the system performance deteriorates (refer to Fig. 3). The starting time of each window is selected blindly. Hence, the proposed system does not require any additional a priori information in implementation. The proposed peak detection receiver utilizes the instantaneous maximum value of signal. Hence, SNR is observed to be higher compared to energy detection receiver.

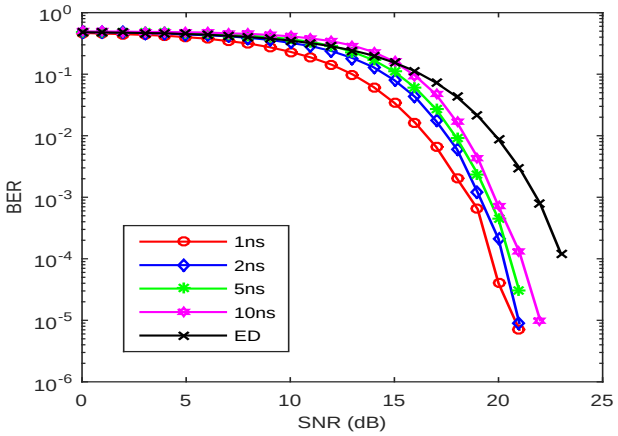

Fig. 3. The average BER performance of TH-PPM UWB system using the proposed receiver and the energy detection receiver in AWGN channel. In above figure, "(·)" ns and "ED" represent the proposed receiver and the energy detection receiver, respectively.

Further, the performance of proposed receiver is analyzed in line-of-sight (LOS) multipath channel model CM1 in residential environment. The channel rms (root mean square) delay of 6.886 ns, frame duration $T_f = 100$ ns and $N_f = 1$ are considered for CM1 channel. The average BER performance of the TH-PPM UWB system in channel model CM1 is shown in Fig. 4. The proposed receiver has better system performance as compared to the energy detector receiver for $T_b = 1$ns as observed from Fig. 4 with low power consumption due to simple hardware implementation. The proposed receiver exploits the instantaneous value of both the desired signal and noise using peak detection circuit. Further, system performance can be improved using the quasi a priori information about the channel $\mathbf{h}$ to obtain the optimum starting time and duration of each window. Therefore, the proposed low power peak detection UWB receiver can be used to connect various devices together in a home environment using IEEE 802.15.4a channel model CM1 [20].

WSN and IoT based applications can operate in non-line-of-sight (NLOS) and dense multipath channel environment [21, 22]. Hence, we have analyzed the proposed receiver performance in non-line-of-sight (NLOS) multipath channel model CM4. The IEEE 802.15.4a channel model CM4 is suitable for analyzing system performance in dense multipath scenario for WSN and IoT in office and large home environment. The average BER performance of the TH-PPM

$$p(e|\mathbf{h}, d_k = 0) = p(\left\{\sum_{i=1}^{M}\left(\prod_{g=1}^{N}\left[1 - Q\left(\frac{s_g + V_{th}}{\sqrt{2\sigma^2 B}}\right) - Q\left(\frac{-s_g + V_{th}}{\sqrt{2\sigma^2 B}}\right)\right]\right)\right\} < \left\{\sum_{i=1}^{M}\left(\prod_{g=1}^{N}\left[1 - 2Q\left(\frac{V_{th}}{\sqrt{2\sigma^2 B}}\right)\right]\right)\right\}). \quad (11)$$

$$p(e|\mathbf{h}, d_k = 1) = p(\left\{\sum_{i=1}^{M}\left(\prod_{g=1}^{N}\left[1 - 2Q\left(\frac{V_{th}}{\sqrt{2\sigma^2 B}}\right)\right]\right)\right\} \geq \left\{\sum_{i=1}^{M}\left(\prod_{g=1}^{N}\left[1 - Q\left(\frac{s_g + V_{th}}{\sqrt{2\sigma^2 B}}\right) - Q\left(\frac{-s_g + V_{th}}{\sqrt{2\sigma^2 B}}\right)\right]\right)\right\}). \quad (12)$$

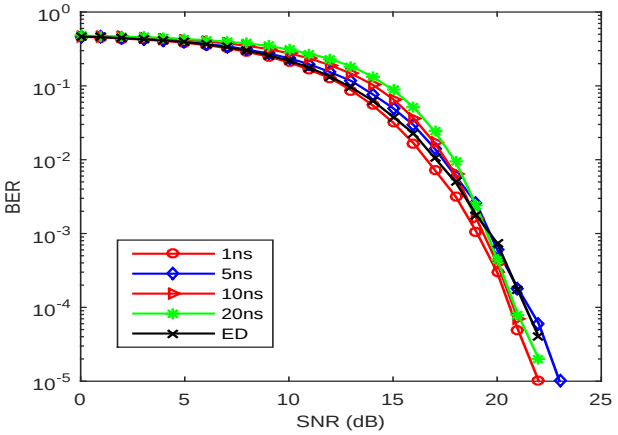

Fig. 4. The average BER performance of TH-PPM UWB system using the proposed receiver and the energy detection receiver in CM1 channel model. In above figure, "(·)" ns and "ED" represent the proposed receiver and energy detection receiver, respectively.

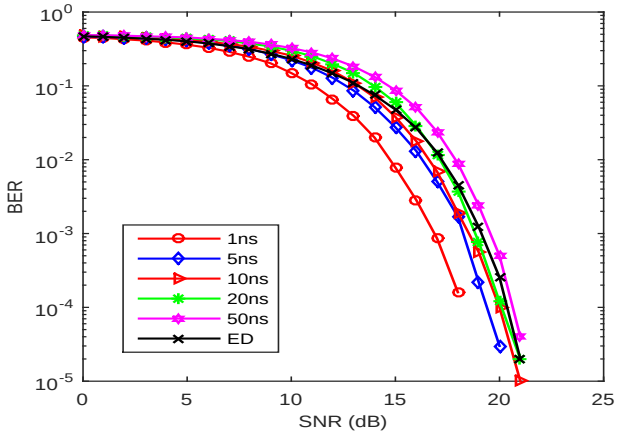

Fig. 5. The average BER performance of TH-PPM UWB system using the proposed receiver and the energy detection receiver in CM4 channel model. In above figure, "(·)" ns and "ED" represent the proposed receiver and energy detection receiver, respectively.

UWB system in channel model CM4 is shown in Fig. 5. The channel rms delay is 24.676 ns using multiple realizations and, frame duration $T_f = 160$ ns and $N_f = 1$ are considered for simulation results. More parameters details can be found in [20]. The proposed non-coherent peak detection receiver yields approximately 1-2 dB performance improvement compared to the energy detection receiver depending upon window time duration T_b as observed from Fig. 5. The relative performance improvement using various window size is almost same for all the values of SNR. Further, from Fig. 4 and Fig. 5, we observe that the TH-PPM UWB system performance in the channel model CM4 is better than the channel model CM1 for both the proposed and energy detection receiver due to more number of multipath. Both channel models CM1 and CM4 are normalized to unity in simulation results.

One reason of performance improvement using the peak value detection is that received multipath signal is sparse in nature, and noise is present through the frame duration. Hence, SNR value at the receiver in energy detector is reduced due to integration over a frame as compared to the proposed peak detection based receiver. Moreover, the proposed peak detection consider only the instantaneous values of signal and noise, hence, its SNR is higher than the energy detector based receiver.

WSN and IoT have many applications in farming and open area surveillance such as border, farm and icing areas. To analyze the performance of the proposed peak detection receiver in open area operating environment, we have used the IEEE 802.15.4a channel model CM9. The CM9 channel rms delay spread is around 30.0428 ns and $T_f = 160$ ns is considered. More details about this channel can be found in [20]. In channel CM9, the transmitted pulse shape is distorted due to frequency depending nature of reflection and diffraction processes. The BER performance using the proposed receiver is better than the energy detector for $T_b = 5, 10$ ns and degrades for window duration $T_b = 1, 2$ ns (around 16-25 dBs SNR range only) as shown in Fig. 6. The BER performance of UWB system is lower in channel CM9 than the CM1 and CM4 channels due to only a few NLOS paths arrival at the receiver, therefore, the effective received signal power is low. Further, the energy detector integrates the energy of the received signal over a frame duration, which mostly contributed by the noise due to the higher sparse nature of the desired signal. The proposed receiver's BER performance degrades in channel CM9 for the lower value of T_b as compared to CM1 and CM4 as shown in Fig. 6, because the probability of presence of the desired signal is low in the small window (time duration). The battery life for IoT applications is more important where power viability or battery replacement is not easily possible such as hilly terrains. Hence, the instance value based proposed peak detector receiver is more useful due to low power consumption in such applications. Further, we observed that the energy detector's performance in more sparsely (less dense) received UWB signal environment degrades, as compared to

the proposed receiver design due to the integration of noise in the decision as observed in the above figures.

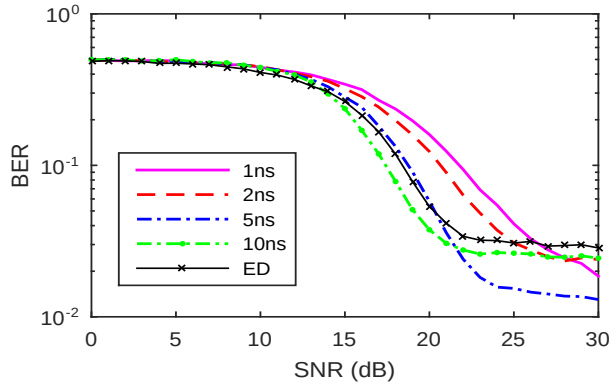

Fig. 6. Average BER performance of TH-PPM UWB system using the proposed receiver and the energy detection receiver in a open area channel model CM9. In above figure, "$(\cdot)$" ns and "ED" represent the proposed receiver and energy detection receiver, respectively.

Implementation: The proposed peak detection receiver can be implemented in analog domain using short analog delay line for small time interval of window T_b at low sampling rate. Also, it can be implemented for long time interval of window T_b ($T_b > 20$ ns) in the discrete domain using high sampling rate ADC (analog-to-digital converter) like energy detector. The discrete implementation of proposed receiver can also be achieved using low sampling rate ADC using compressive sensing method. The power consumption of peak detector is smaller than the energy detector [23]. A complete power analysis of the proposed peak detection receiver and comparison with energy detection will be taken up in the near future. The computational complexity of peak and energy detection algorithms is $O(\log n)$ and $2O(n)$, respectively. The simulation time for both the peak and energy detection receiver in MATLAB on an Intel(R) Core(TM) i7-4790 CPU @ 3.6GHz with 8 GB RAM and 64 bit operating system was observed to be 4.2365 and 6.5622 minutes, respectively, for 100 data frames and ensemble average of 100 realizations.

V. Conclusion

In this paper, we have proposed a simple peak detection based non-coherent UWB receiver for WSN and IoT based applications. The proposed receiver performance for TH-PPM UWB system is analyzed in AWGN, and multipath channels using IEEE 802.15.4a standard. The proposed receiver has better system performance as compared to the energy detector receiver with low power consumption and less system implementation complexity. In the near future, the weighted summation of peak detection probabilities in each window duration can be analyzed for improved system performance.

References

[1] D. Morche, "UWB returns as a GPS for IoT: Impulse radio enables indoor location apps," EE|Times, 18 Nov. 2014.

[2] Z. Zou, "Impulse radio UWB for the internet-of-things: A study on UHF/UWB hybrid solution," Ph.D. dissertation, KTH School of Information and Communication Technology, SE-164 40 Kista, Stockholm Sweden, Nov. 2011.

[3] B. Lewis, "UWB is back ... this time for IoT location-based services," Embedded Computing Design, 15 Oct. 2014.

[4] Z. Zou, D. S. Mendoza, P. Wang, Q. Zhou, J. Mao, F. Jonsson, H. Tenhunen, and L.-R. Zheng, "A low-power and flexible energy detection IR-UWB receiver for RFID and wireless sensor networks," *IEEE Transactions on Circuits and Systems I: Regular Papers*, vol. 58, no. 7, pp. 1470–1482, 2011.

[5] N. Decarli, F. Guidi, and D. Dardari, "Passive UWB RFID for tag localization: Architectures and design," *IEEE Sensors Journal*, vol. 16, no. 5, pp. 1385–1397, Mar. 2016.

[6] A. Bekasiewicz and S. Koziel, "Compact UWB monopole antenna for internet of things applications," *Electronics Letters*, vol. 52, no. 7, pp. 492–494, 2016.

[7] M. Viot, "Decawave sees UWB and micro-location in 2015's internet of things," Decawave Technology, 2015.

[8] S. Harrison and P. F. Driessen, "Novel UWB and spread spectrum system using time compression and overlap-add techniques," *IEEE Access*, vol. 2, pp. 1092–1105, 2014.

[9] N. Rendevski and D. Cassioli, "60 GHz UWB rake receivers in a realistic scenario for wireless home entertainment," in *IEEE International Conference on Communications (ICC)*, 2015, pp. 2744–2749.

[10] D. Dardari, R. D'Errico, C. Roblin, A. Sibille, and M. Z. Win, "Ultra-wide bandwidth RFID: The next generation?" *Proceedings of the IEEE*, vol. 98, no. 9, pp. 1570–1582, 2010.

[11] K. Witrisal, G. Leus, G. J. Janssen, M. Pausini, F. Trösch, T. Zasowski, and J. Romme, "Noncoherent ultra-wideband systems," *IEEE Signal Processing Magazine*, vol. 26, no. 4, pp. 48–66, 2009.

[12] X. Cheng, Y. L. Guan, and S. Li, "Optimal BER-balanced combining for weighted energy detection of UWB OOK signals," *IEEE Communications Letters*, vol. 17, no. 2, pp. 353–356, 2013.

[13] F. Wang, Z. Tian, and B. M. Sadler, "Weighted energy detection for noncoherent ultra-wideband receiver design," *IEEE Transactions on Wireless Communications*, vol. 10, no. 2, pp. 710–720, 2011.

[14] S. Nagaraj and F. Rassam, "Improved non-coherent UWB receiver for implantable biomedical devices," *IEEE Transactions on Biomedical Engineering*, vol. PP, no. 99, 2015.

[15] A. Vizziello and P. Savazzi, "Efficient RFID tag identification exploiting hybrid UHF-UWB tags and compressive sensing," *IEEE Sensors Journal*, vol. 16, no. 12, pp. 4932–4939, 2016.

[16] H. W. Pflug, J. Romme, K. Philips, and H. de Groot, "Method to estimate impulse-radio ultra-wideband peak power," *IEEE Transactions on Microwave Theory and Techniques*, vol. 59, no. 4, pp. 1174–1186, 2011.

[17] K. Allidina, T. Khattab, and M. N. El-Gamal, "On dual peak detection UWB receivers in noise and interference dominated environments," *AEU-International Journal of Electronics and Communications*, vol. 70, no. 2, pp. 121–131, 2016.

[18] M. Ghavami, A. Amini, and F. Marvasti, "Unified structure of basic UWB waveforms," *IEEE Transactions on Circuits and Systems II: Express Briefs*, vol. 12, no. 55, pp. 1304–1308, 2008.

[19] A. Gerosa, S. Soldà, A. Bevilacqua, D. Vogrig, and A. Neviani, "An energy-detector for noncoherent impulse-radio UWB receivers," *IEEE Transactions on Circuits and Systems I: Regular Papers*, vol. 56, no. 5, pp. 1030–1040, 2009.

[20] A. F. Molisch, D. Cassioli, C.-C. Chong, S. Emami, A. Fort, B. Kannan, J. Karedal, J. Kunisch, H. G. Schantz, K. Siwiak *et al.*, "A comprehensive standardized model for ultrawideband propagation channels," *IEEE Transactions on Antennas and Propagation*, vol. 54, no. 11, pp. 3151–3166, 2006.

[21] B. Silva and G. P. Hancke, "IR-UWB-based non-line-of-sight identification in harsh environments: Principles and challenges," *IEEE Transactions on Industrial Informatics*, vol. 12, no. 3, pp. 1188–1195, 2016.

[22] M. Cheffena, "Industrial wireless sensor networks: channel modeling and performance evaluation," *EURASIP Journal on Wireless Communications and Networking*, vol. 2012, no. 1, pp. 1–8, 2012.

[23] L. Liu, Y. Miyamoto, Z. Zhou, K. Sakaida, J. Ryu, K. Ishida, M. Takamiya, and T. Sakurai, "A 100Mbps, 0.19 mW asynchronous threshold detector with DC power-free pulse discrimination for impulse UWB receiver," in *IEEE Proceedings of the 2009 Asia and South Pacific Design Automation Conference*, 2009, pp. 97–98.